

1 **Microbial necromass contribution to topsoil organic carbon storage of natural**
2 **and agricultural ecosystems**

3
4 Jing-li Lu^a, Thomas W. Crowther^b, Manuel Delgado-Baquerizo^c, Wenjie Liu^a, Yamin
5 Jiang^a, Hongyang Sun^d, Zhiqiang Wang^{d, *}

6
7 ^a Hainan Baoting Tropical Forest Ecosystem Observation and Research Station,
8 School of Ecology, Hainan University, Haikou, 570228, People's Republic of China;

9 ^b Institute of Integrative Biology, Department of Environmental Systems Science,
10 ETH Zürich, 8092 Zürich, Switzerland;

11 ^c Laboratorio de Biodiversidad y Funcionamiento Ecosistémico, Instituto de Recursos
12 Naturales y Agrobiología de Sevilla (IRNAS), CSIC, Seville, 41013, Spain;

13 ^d Sichuan Zoige Alpine Wetland Ecosystem National Field Observation and Research
14 Station, College of Grassland Resources, Southwest Minzu University, Chengdu,
15 610041, People's Republic of China

16
17
18 * Corresponding author: Zhiqiang Wang

19 *E-mail address:* wangzq@swun.edu.cn

20

21 **Abstract**

22 Microbial necromass is an important component of soil carbon (C). Yet, the relative
23 contribution of microbial necromass in shaping the global C stocks in agricultural and
24 natural ecosystems worldwide remains virtually unknown. Here, we compiled data on
25 fungal and bacterial necromass along with soil organic carbon (SOC) from the 0–20
26 cm soil layer across 486 study sites (145 agricultural and 341 natural ecosystems) to
27 evaluate the relative contribution of fungal necromass C (FNC) and bacterial
28 necromass C (BNC) to SOC. Our results indicated that, on average, FNC is two times
29 more important than BNC in explaining SOC in both agricultural and natural
30 ecosystems. The contributions of FNC and BNC to SOC were markedly higher in
31 agricultural ecosystems compared with natural ecosystems, with a contrasting trend in
32 the FNC/BNC ratio. Soil physicochemical properties (soil C/N ratio and clay content)
33 were the most important predictors of the contributions of FNC and BNC to SOC in
34 both ecosystems, while geographical factor (elevation) was the most important
35 predictor of the FNC/BNC ratio. Our study enhances the current level of
36 understanding regarding microbially mediated biogeochemical cycling and SOC
37 dynamics, underscoring the critical role of microbial necromass in the global C cycle.

38
39 **Keywords:** agricultural ecosystems, bacterial necromass carbon, fungal necromass
40 carbon, microbial necromass carbon, natural ecosystems

41 42 **1 Introduction**

43 As the largest carbon (C) pool in the terrestrial biosphere, soil organic carbon (SOC)
44 plays a pivotal role in shaping the global C cycle and climate system (Bellamy et al.,
45 2005; Crowther et al., 2015). In brief, plant inputs provide the primary carbon source
46 to soils, and microbial processing transforms these inputs into microbial necromass
47 that can persist over long turnover times (Cotrufo et al., 2013; Angst et al., 2021).
48 Although the living soil microbial biomass typically constitutes only about 2% of
49 SOC (a ratio referred to as the microbial quotient; Anderson & Domsch, 1989; Liu et
50 al., 2023), microbial necromass has been shown to contribute more than half and up to
51 approximately 80% of SOC, depending on soil type and analytical methods (Liang &
52 Balser, 2011; Kallenbach et al., 2016; Liang et al., 2019). In other words, microbial
53 necromass C (MNC) constitutes a substantial and critical component of stable SOC
54 (Ma et al., 2018), and its dynamics are increasingly recognized for their role in
55 regulating the terrestrial carbon cycle and climate feedbacks (Zhao et al., 2023). As
56 such, there is growing scientific attention on the forces driving the accumulation of
57 MNC and its contribution to SOC (Liang et al., 2017; Ni et al., 2020; Luo et al., 2022;
58 Zhou et al., 2023). To gain a comprehensive understanding of MNC in the global C
59 cycle, recent research has highlighted the distinct roles of fungal and bacterial
60 necromass, revealing their contrasting responses to environmental and anthropogenic
61 drivers. For instance, studies have shown that the accumulation and contribution of
62 MNC are sensitive to factors such as aridity, primary productivity, agricultural
63 management practices like tillage and fertilization, as well as key soil properties
64 including pH and clay content (Zhang et al., 2021; Zhou et al., 2023; Xu et al., 2024).

65 Despite these advances, it remains unclear whether these organism-specific
66 mechanisms translate into systematic differences in necromass contributions between
67 ecosystems under varying degrees of human interference, such as agricultural versus
68 natural systems.

69 With the distinct roles of fungi and bacteria in decomposing organic matter and
70 stabilizing organic carbon in soil, the relative contribution to SOC of fungal and
71 bacterial necromass C could be used to track the dynamics of SOC storage (Malik et
72 al., 2016). The cell walls of fungi primarily consist of chitin (a nitrogen-containing
73 polysaccharide) and β -glucans, whereas bacterial cell walls are mainly composed of
74 peptidoglycan—a complex of sugars and amino acids (Lenardon et al., 2007). As
75 bacterial amino sugars are readily degradable, while fungal chitin and -glucans are
76 more recalcitrant, fungal necromass generally exhibits a longer turnover time in soil
77 compared to bacterial necromass (Xu et al., 2022). Wang et al. (2021a) reported that
78 the contribution of fungal necromass carbon (FNC) to SOC exceeded 65%,
79 considerably higher than that of bacterial necromass carbon (BNC, 32–36%). This
80 pattern is likely attributed to the slower decomposition rate and stronger
81 mineral-associative capacity of fungal necromass. Furthermore, greater fungal
82 biomass and higher turnover rates may enhance the input flux of fungal necromass
83 (Klink et al., 2022). The contributions of FNC and BNC to SOC depended on the type
84 of ecosystems (Wang et al., 2021a; Cao et al., 2023; Xu et al., 2024). However, few
85 studies on fungal and bacterial necromass carbon and their contribution to SOC has
86 been reported for ecosystems under human interference (Zhou et al., 2023).

87 Terrestrial ecosystems can be broadly categorized into managed (agricultural) and
88 natural ecosystems (Hobbs et al., 2011; Keith et al., 2022). The agricultural
89 ecosystems are typical of plant litter derived from single crops under intensive human
90 management (Bohan et al., 2013), a context that typically leads to bacterial-dominated
91 soil communities (van Der Heijden et al., 2008). In contrast, natural ecosystems
92 display greater diversity in plant litter and root deposits (Wu et al., 2019). In such
93 ecosystems, fungal mycelial networks and stable soil aggregates are enhanced,
94 leading to higher FNC contributions to SOC (Sanaullah et al., 2020; Sae-Tun et al.,
95 2022). While bacteria are undoubtedly vital decomposers, fungi play a distinct and
96 often dominant role in the initial breakdown of complex plant polymers such as
97 cellulose and lignin. This functional prominence stems from their potent enzymatic
98 machinery and hyphal growth form, which enable physical penetration and decay of
99 solid organic matter (de Boer et al., 2005). As key decomposers, fungi are thus critical
100 in processing cellulose and other complex organic compounds (Hättenschwiler et al.,
101 2005). Accordingly, as demonstrated by Choi et al. (2018), soil cellulose-degrading
102 genes are frequently linked to fungal activity and abundance. Rather than implying
103 higher cellulose concentration per se, diverse plant inputs increase the chemical
104 heterogeneity of plant-derived polymers (e.g., cellulose, hemicelluloses, and lignin),
105 which broadens decomposer niches and often favors fungal communities in litter
106 horizons (Hättenschwiler et al., 2005; Štursová et al., 2012). In contrast, agricultural
107 monocultures tend to reduce fungal diversity unless mitigated by management
108 practices (Chen et al., 2020). Reflecting this context dependence, cellulose-rich inputs

109 can enrich saprotrophic fungi in arable soils (Clocchiatti et al., 2021), whereas
110 bacteria may contribute substantially in mineral soils or under specific microhabitat
111 and land management conditions (Štursová et al., 2012; Choi et al., 2018). Due to
112 distinct chemical properties and organo-mineral stabilization pathways, fungal and
113 bacterial necromass exhibit differing turnover times, making the FNC/BNC ratio a
114 mechanistic tracer of SOC formation (Angst et al., 2021; Kleber et al., 2021).
115 Therefore, elucidating the global distribution and drivers of FNC, BNC, and their ratio
116 across agricultural and natural ecosystems is essential for predicting
117 management-induced shifts in SOC under varying climatic and soil conditions (Zhang
118 et al., 2021; Zhou et al., 2023; Xu et al., 2024).

119 In order to explore the global patterns and drivers of FNC, BNC and the
120 FNC/BNC ratio in agricultural and natural ecosystems, we compiled data from 486
121 study sites worldwide. The aims of this study were: (1) to quantify the contributions
122 of FNC and BNC to SOC and the FNC/BNC ratio in agricultural and natural
123 ecosystems; and (2) to investigate the primary driving factors influencing the
124 contributions of FNC and BNC to SOC and the FNC/BNC ratio.

125

126 **2 Materials and methods**

127 2.1 Data collection

128 We compiled a comprehensive dataset following the stepwise workflow. (1) We
129 collected peer-reviewed papers published from 1996 to 31 December 2022 from Web
130 of Science (<http://apps.webofknowledge.com>), Google Scholar
131 (<http://scholar.google.com>), and the China National Knowledge Infrastructure
132 (<http://cnki.net>), using the keywords: ‘amino sugars’, ‘microbial necromass’,
133 ‘microbial residue’, ‘fungal residue’, and ‘bacterial residue’. Records from different
134 databases were merged and deduplicated to form an initial compilation. (2) We then
135 filtered the compiled studies to include only those focusing on topsoil, defined as the
136 0–20 cm layer. Studies reporting deeper or unspecified sampling depths (e.g., 0–30
137 cm) were excluded to ensure spatial comparability. (3) Full texts were assessed to
138 confirm the presence of paired fungal and bacterial residue data from the same
139 sample—specifically, glucosamine (GluN) and muramic acid (MurA), or directly
140 reported FNC and BNC values—to enable consistent cross-study calculation of the
141 FNC/BNC ratio. Studies lacking either biomarker were excluded from ratio analyses,
142 though those directly reporting the FNC/BNC ratio were retained. (4) Eligible
143 observations were classified into agricultural ecosystems (including dry land, irrigated
144 cropland, and submerged paddy) or natural ecosystems (forest and grassland) based
145 on study metadata. (5) For natural ecosystems, data from fertilized, polluted,
146 experimentally treated, or otherwise anthropogenically disturbed sites were excluded.
147 In total, the final dataset consisted of 2094 observations from 486 sites worldwide
148 (145 agricultural and 341 natural sites; Figure 1) reported in 164 peer-reviewed papers.
149 Of these observations, 1001 were from agricultural ecosystems, and 1093 from natural
150 ecosystems. Among the 341 natural sites, 195 were forests and 146 were grasslands.
151 For agricultural sites, we used Google Earth Engine with the LGRIP30 V1 dataset to
152 classify agricultural ecosystem into dry land and irrigated cropland, and we overlaid

153 the JRC surface-water seasonality layer to extract submerged paddy from the irrigated
154 class (LGRIP30 irrigated value = 2 and JRC seasonality ≥ 1). We ultimately classified
155 145 samples of agricultural ecosystems into 32 dry land, 72 irrigated, and 41
156 submerged paddy sites.

157 We calculated the FNC and BNC based on amino sugar concentrations following
158 widely used conversion factors, correcting total GluN for its bacterial share using
159 MurA:

$$160 \quad FNC = \left(\frac{GluN}{179.17} - 2 \times \frac{MurA}{251.23} \right) \times 179.17 \times 9 \quad \text{Equation 1}$$

161 where 9 (unitless) is the conversion factor from GluN to FNC. To estimate
162 fungal-derived GluN, we subtracted the bacterial share of GluN assuming an
163 empirical GluN:MurA molar ratio of 2:1 for bacterial residues. 179.17 and 251.23 are
164 the molecular weights of GluN and MurA, respectively. And their units are all g/mol.
165 The unit of FNC is mg/kg.

$$166 \quad BNC = MurA \times 45 \quad \text{Equation 2}$$

167 where 45 (unitless) is the conversion factor from MurA to BNC. The unit of BNC
168 is mg/kg.

169 Additional information including site geographic location (latitude and longitude),
170 topographical condition (elevation), climatic factors (mean annual temperature [MAT]
171 and mean annual precipitation [MAP]), soil physicochemical properties (pH, SOC,
172 total nitrogen [TN], clay content, and soil temperature), and biotic (microbial and
173 plant) factors were recorded. Specifically, biotic factors included microbial biomass
174 carbon (MBC), microbial biomass nitrogen (MBN), MBC/MBN, net primary
175 production (NPP), and belowground biomass C density (BGBC). The data of
176 topographical condition (elevation) was classified as geographical factor in this study.
177 When MAT and MAP were unavailable in the original articles, we extracted them
178 from the global climate layers of WorldClim (<http://www.worldclim.org/>) with a grid
179 precision of 30×30 arc sec according to geographic location. Missing elevation data
180 were extracted using the *elevatr* package v.0.4.2 (Hollister, 2021) in the R
181 environment. We acquired the data on annual mean soil temperature from the study of
182 Lembrechts et al. (2022), while other absent soil physicochemical data were extracted
183 from the Harmonized World Soil Database
184 (<https://www.fao.org/soils-portal/data-hub/soil-maps-and-databases/harmonized-world-soil-database-v12/en/>)
185 and SoilGrids 2.0 (Poggio et al., 2021;
186 <https://www.soilgrids.org/>) using ArcGIS 10.3. We supplemented missing climatic and
187 soil variables using high-resolution, globally interpolated datasets to ensure consistent
188 spatial coverage across all sites. After retrieving missing value from gridded data, we
189 typically calibrate them against field-reported values via a field-anchored bias
190 correction (i.e., a site- or region-specific “delta” adjustment) to minimize errors
191 introduced by gridded data. While the use of such data introduces inherent
192 uncertainties, these databases are widely adopted in global-scale ecological analyses
193 and provide the most feasible approach for a unified assessment. In addition, the data
194 on NPP and BGBC were acquired from the studies of Zhao and Running (2010) and
195 Spawn et al. (2020), respectively. Missing MBC and MBN data were acquired using a

196 global database with a high resolution of 30×30 arc sec (Wang et al., 2022).

197

198 2.2 Statistical analysis

199 All the statistical analyses were performed using R v4.1.3 (R Core Team, 2021).
200 Initially, the Shapiro–Wilk test was employed to assess the normality of our data,
201 followed by the application of Levene's test to evaluate the homogeneity of variances
202 across different groups. To detect the significant differences in the contributions of
203 FNC and BNC to SOC, and the FNC/BNC ratio between agricultural and natural
204 ecosystems, as well as between forest and grassland ecosystems, the Wilcoxon rank
205 sum test was conducted. Kruskal–Wallis and Dunn's post hoc tests were used to
206 assess the significant differences of the contributions of FNC and BNC to SOC, and
207 the FNC/BNC ratio among dry land, irrigated cropland, and submerged paddy. We
208 used Spearman's rank correlation coefficient to explore the connections between the
209 16 variables considered in this study, including geographical and climatic factors, soil
210 physicochemical properties, and biotic factors. Since there was a strong positive
211 correlation between MAT and soil temperature (Figure S1), soil temperature was
212 excluded from our subsequent analyses. Linear regressions between different factors
213 and the contributions of FNC and BNC to SOC and the FNC/BNC ratio were
214 performed. Dots and smoothing curves were drawn using the *geom_point* and
215 *geom_smooth* functions, respectively, in the *ggplot2* package v.3.4.0 (Wickham,
216 2016).

217 Variation partitioning analysis was conducted using the *vegan* package v.2.5.7
218 (Oksanen et al., 2020) to evaluate the effects of four types of factors on the
219 contributions of FNC and BNC to SOC and the FNC/BNC ratio in agricultural and
220 natural ecosystems at global scale. We used a variance inflation factor threshold of 3.3
221 to eliminate those variables that were strongly correlated and avoid multicollinearity
222 (Figure S2; Kock, 2015; Fanin et al., 2020). Following factor selection, boosted
223 regression trees (BRTs) were used to partition independent influences of geographical
224 (elevation) and climatic (MAT and MAP) factors, soil physicochemical properties (pH,
225 clay, C/N, and SOC), and biotic factors (NPP, BGBC, MBC, and MBC/MBN) on the
226 contributions of FNC and BNC to SOC and the FNC/BNC ratio with the *gbm* package
227 v.2.1.8.1 (Greenwell et al., 2022).

228 Utilizing the selected factors, we performed structural equation models (SEMs)
229 to quantify the effects (direct, indirect and both) of four types of factors on the
230 contributions of FNC and BNC to SOC and the FNC/BNC ratio using *lavaan* package
231 v.0.6.19 (Rosseel, 2012). According to the previously reported potential causal
232 relationships between explanatory and response variables (Wang et al., 2021a, 2021b;
233 Li et al., 2024), we established the *priori* structural equation models for agricultural
234 and natural ecosystems, respectively (Figure S3). The SEMs were fitted via maximum
235 likelihood estimation, with non-significant paths iteratively pruned through stepwise
236 exclusion, followed by model evaluation using modification indices and
237 goodness-of-fit criteria. The fit indices included degrees of freedom (df), chi-square
238 (χ^2 , $0 \leq \chi^2/\text{df} \leq 2$), comparative fit index (CFI > 0.9), and root mean square error of
239 approximation (RMSEA < 0.08), which were used to assess the adequacy of the SEM.

240 Map, box, bar, bubble, and lollipop charts were plotted with the *ggplot2* package
241 v.3.4.0 (Wickham, 2016). To enhance map visualization, the *ggnewscale* package
242 v.0.4.8 (Campitelli, 2022) was necessary alongside the *ggplot2* package v.3.4.0
243 (Wickham, 2016). Similarly, the *ggpubr* package v.0.5.0 (Kassambara, 2022) was an
244 additional necessity when creating lollipop charts.

245

246 **3 Results**

247 3.1 Fungal and bacterial necromass contribution to SOC in agricultural and natural 248 ecosystems

249 Our analysis revealed statistically significant disparities in the contributions of FNC
250 and BNC to SOC in agricultural and natural ecosystems at the global scale ($P < 0.05$;
251 Figure 2a, b). Notably, the average contributions of FNC and BNC to SOC were
252 substantially higher in agricultural ecosystems than in natural ecosystems ($P < 0.001$;
253 Figures 2a, b). For FNC, the average contribution was 34.39% in agricultural
254 ecosystems, versus 29.24% in natural ecosystems. BNC contributed an average of
255 15.65% to SOC in agricultural ecosystems, compared to 14.02% in natural
256 ecosystems (Table 1). Our results also indicated that the contributions of FNC to SOC
257 were approximately twice those of BNC in agricultural and natural ecosystems (Table
258 1).

259 The contributions of FNC and BNC to SOC indicated no significant difference
260 between dry land and irrigated cropland ($P > 0.05$), whereas both differed
261 significantly from submerged paddy ($P < 0.05$; Figure S4a, b). In detail, across dry
262 land, irrigated cropland, and submerged paddy, the mean contributions of FNC to
263 SOC were 37.77%, 35.35%, and 22.82%, respectively, whereas those of BNC were
264 17.34%, 15.95%, and 10.55% (Table 1). Moreover, there were no significant
265 differences in the contributions of FNC and BNC to SOC between forest and
266 grassland ecosystems ($P > 0.05$; Figure S5). Specifically, FNC contributed, on
267 average, 29.11% to SOC in forests and 26.75% in grasslands, while BNC contributed
268 13.48% in forests and 14.34% in grasslands (Table 1).

269

270 3.2 Ratios of fungal and bacterial necromass in agricultural and natural ecosystems

271 Our results indicated that, at the global scale, the soil FNC/BNC ratio differs
272 significantly between agricultural and natural ecosystems ($P < 0.05$; Fig. 2c), with a
273 higher ratio in natural ecosystems (3.22) than in agricultural ecosystems (2.61; Table
274 1). The FNC/BNC ratio did not differ significantly among dry land, irrigated cropland,
275 and submerged paddy ($P > 0.05$; Figure S4c), with average FNC/BNC ratios of 2.87,
276 2.51, and 2.62, respectively (Table 1). Similarly, there was no significant difference in
277 the FNC/BNC ratio between forest and grassland ecosystems ($P > 0.05$; Figure S5),
278 and the average FNC/BNC ratios for forests and grasslands were 2.80 and 3.58 (Table
279 1), respectively.

280

281 3.3 Associations of abiotic and biotic factors with microbial necromass parameters

282 Soil physicochemical factors were the most important influence on the contributions
283 of FNC and BNC to SOC across both ecosystem types (Figures 3a–d, 4a–d).

284 Specifically, they explained 16% and 17% of the variance in the contributions of FNC
285 and BNC to SOC in agricultural ecosystems, respectively (Figures 3a, c), and 20%
286 and 24% in natural ecosystems (Figures 3b, d). BRTs corroborated this pattern, with
287 soil physicochemical factors showing the highest relative influence (51% for FNC,
288 and 44% for BNC) in agricultural systems and 44% in natural systems (Figures 4a–d).
289 All BRT models were significant ($P < 0.001$), with explained variance 36–66%. While
290 soil factors dominated overall, responses to individual variables differed between
291 ecosystems. In detail, in agricultural systems, the C/N ratio ranked third for FNC after
292 clay and SOC (Figure 4a), whereas C/N was the top predictor for FNC in natural
293 systems and for BNC in both ecosystems (Figures 4b–d). Consistently, linear models
294 showed declines in the contributions of FNC and BNC with increasing C/N in both
295 ecosystems (Figures S6g, S7g). SEMs yielded convergent results, indicating both
296 direct and indirect pathways (Figures 5a–d, 6a–d). Notably, the direct and total effects
297 of soil physicochemical factors on FNC were negative in agricultural but positive in
298 natural ecosystems (Figures 5a, b, 6a, b), whereas the effects on BNC were negative
299 in both ecosystem types (Figures 5c, d, 6c, d).

300 Our results indicated that geographical factors were the most important
301 contributors to explain the FNC/BNC ratio in both agricultural and natural ecosystems,
302 accounting for 21% and 10% of the explained variance in the FNC/BNC ratio,
303 respectively (Figures 3e, f). The results of the BRTs suggested that geographical
304 factors played a similar role in explaining the FNC/BNC ratio (Figures 4e, f). In the
305 BRT models, geographical factors emerged as the primary influencers of the
306 FNC/BNC ratio in agricultural and natural ecosystems, accounting for 32% and 44%
307 of the variance in each case, respectively (Figures 4e, f). To be more specific,
308 elevation was the most significant geographical factors influencing the FNC/BNC
309 ratio in both ecosystems (Figures 4e, f). Moreover, the FNC/BNC ratio in agricultural
310 and natural ecosystems show significantly increased with an increase elevation
311 (Figure S8a). The results of SEMs also indicated that geographical factors were the
312 most influential factors for the FNC/BNC ratio in agricultural and natural ecosystems,
313 exerting both direct and indirect effects on this ratio (Figures 5e, 6e), with the
314 standardized total effect being positive (Figures 5f, 6f).

315

316 **4 Discussion**

317 **4.1 Fungal necromass contributes two times more to SOC than bacterial necromass**

318 Our results show that in agricultural ecosystems, FNC/SOC ranged from 0.09% to
319 97.53% (mean \pm SE: $34.39 \pm 0.67\%$), and BNC/SOC ranged from 0.81% to 65%
320 ($15.65 \pm 0.33\%$). In natural ecosystems, FNC/SOC ranged from 0.92% to 96.29%
321 ($29.24 \pm 0.51\%$), and BNC/SOC ranged from 0.25% to 89.45% ($14.02 \pm 0.36\%$)
322 (Table 1). The FNC/BNC ratio ranged from 0.02 to 12.74 (2.61 ± 0.06) in agricultural
323 ecosystems and from 0.12 to 44.24 (3.22 ± 0.11) in natural ecosystems (Table 1).
324 Despite substantial variability at the individual sample level, the mean contribution of
325 FNC was approximately twice that of BNC in both ecosystem types. Moreover, the
326 mean FNC/BNC ratio was significantly higher in natural ecosystems than in
327 agricultural ecosystems ($P < 0.05$; Figure 2). Although this general pattern has been

328 reported in previous studies (Liang et al., 2019; Wang et al., 2021a; Zhang et al., 2023;
329 Ding et al., 2024), the systematic differences in the magnitude of these contributions
330 between agricultural and natural ecosystems—and their underlying drivers—have
331 remained poorly understood. Our study not only confirms the broad pattern but also
332 elucidates these ecosystem-level disparities and their environmental determinants.
333 Consistent with our finding that the contribution of fungal necromass carbon (FNC) to
334 SOC exceeded that of bacterial necromass carbon (BNC) in both ecosystem types
335 (Table 1), the predominance of fungal necromass may be attributed to its more
336 recalcitrant cell wall composition (e.g., chitin) and slower decomposition rate (Wang
337 et al., 2021a). Our BRT and SEM analyses further identified soil clay content and C/N
338 ratio as key drivers of FNC accumulation (Figs. 4a, 5a), reinforcing the importance of
339 organo-mineral associations in the stabilization of fungal-derived carbon.

340 Additionally, our study reveals previously unreported disparities between
341 ecosystem types, for example, the contributions of both fungal and bacterial
342 necromass carbon (FNC and BNC) to SOC were significantly higher in agricultural
343 ecosystems, while the FNC/BNC ratio was substantially elevated in natural
344 ecosystems. The higher contributions of FNC and BNC to SOC in agricultural
345 ecosystems may be attributable to two main factors. First, natural ecosystems
346 typically receive larger and more heterogeneous plant-derived carbon inputs than
347 agricultural systems. These inputs expand the plant-derived SOC pool and can dilute
348 the relative contribution of microbial necromass to SOC, thereby resulting in a lower
349 perceived contribution of microbial necromass in natural ecosystems (Angst et al.,
350 2021; Kleber et al., 2021). Second, the significantly lower soil C/N ratio in
351 agricultural ecosystems (10.78) compared to natural ecosystems (27.44) reflects
352 relative nitrogen enrichment, largely resulting from anthropogenic fertilization
353 (Castellano et al., 2015; Chen et al., 2020). This nitrogen-rich environment can
354 enhance microbial carbon use efficiency and alleviate nutrient limitation, thereby
355 promoting the production and accumulation of microbial necromass (Liang et al.,
356 2017). Supporting this mechanism, we found that the contributions of both FNC and
357 BNC to SOC decreased significantly with increasing soil C/N ratio in both
358 agricultural ecosystems (FNC/SOC: $R = -0.27$, $P < 0.001$; BNC/SOC: $R = -0.29$, $P <$
359 0.001) and natural ecosystems (FNC/SOC: $R = -0.17$, $P < 0.001$; BNC/SOC: $R =$
360 -0.35 , $P < 0.001$; Figures S6g, S7g). These results further underscore that a lower soil
361 C/N ratio—often indicative of higher nitrogen availability—is a key driver of
362 microbial necromass accumulation. It should be noted that although in situ plant
363 residues in agricultural systems (e.g., cereal straw) may have high C/N ratios, the
364 overall soil C/N ratio is reduced by management practices such as mineral fertilization
365 and the incorporation of low C/N organic amendments.

366 Furthermore, nutrient-rich conditions prevalent in agricultural systems (e.g., due
367 to fertilization) often select for bacterial-dominated communities, as many bacteria
368 exhibit *r*-strategist traits that support rapid growth under high resource availability. In
369 contrast, natural ecosystems—characterized by lower nutrient availability and greater
370 resource heterogeneity—tend to favor fungal dominance, since fungi often function as
371 *K*-strategists with higher efficiency in decomposing complex organic matter under

372 resource-limited conditions (Strickland & Rousk, 2010; Yu et al., 2022). This shift in
373 microbial community composition is observed in our results, which show a
374 significantly higher FNC/BNC ratio in natural ecosystems across our global dataset
375 (Figure 2c, Table 1). A high FNC/BNC ratio signifies a fungal-dominated
376 decomposition pathway. Fungal necromass—rich in recalcitrant compounds such as
377 chitin—is more resistant to decay, and fungal hyphae play a key role in the formation
378 of stable soil aggregates that physically protect organic matter from degradation
379 (Lenardon et al., 2007). This pathway promotes the formation of stable, long-turnover
380 SOC pools essential for long-term carbon sequestration (Six et al., 2006; Lehmann et
381 al., 2020). Furthermore, fungi generally exhibit higher carbon use efficiency than
382 bacteria, meaning a larger proportion of assimilated carbon is allocated to biomass
383 production (and subsequently necromass) rather than being respired as CO₂ (Wang &
384 Kuzyakov, 2024). Thus, the fungal-driven pathway characteristic of natural
385 ecosystems represents a highly efficient conversion of plant litter into persistent soil
386 organic matter (Kallenbach et al., 2016; Malik et al., 2016). Conversely, the lower
387 FNC/BNC ratio observed in agricultural ecosystems reflects a bacterial-dominated
388 pathway, accelerated by practices such as tillage and nutrient amendments. This
389 pathway is associated with faster carbon cycling and greater carbon loss through
390 respiration. Although microbial necromass can accumulate under these
391 conditions—sometimes contributing more significantly to a reduced total SOC
392 pool—the resulting carbon is often less stabilized (Zhou et al., 2023). Therefore, the
393 FNC/BNC ratio serves not merely as a descriptive metric, but as a functional
394 biomarker that elucidates fundamental differences in the stability and persistence of
395 SOM between managed agricultural systems and natural ecosystems.

396 Notably, as major components of agricultural ecosystems, both dryland and
397 irrigated croplands exhibited significantly greater contributions of FNC and BNC to
398 SOC than submerged paddy soils, although the FNC/BNC ratio did not differ
399 significantly among these three systems (Figure S4). This pattern may reflect similar
400 aeration regimes in dryland and irrigated systems (predominantly oxygenated),
401 leading to comparable decomposition–transformation–mineral association pathways
402 and, thus, similar net contributions of fungal and bacterial residues to SOC
403 (Ghezzehei et al., 2019). By contrast, persistent or periodic flooding in paddy soils
404 induces anoxia, suppresses aerobic decomposition, and shifts metabolic pathways
405 (e.g., denitrification and methanogenesis), potentially suppressing fungal activity or
406 dominance and altering the relative accumulation and turnover of fungal and bacterial
407 necromass (Qiu et al., 2017), resulting in contributions that differ significantly
408 from—and are lower than—those in the other two systems. Flooding can suppress
409 fungi yet also enhance the joint retention of both fungal and bacterial necromass via
410 slower decomposition and mineral protection, yielding unchanged ratios but altered
411 totals or compositional pathways (Chen et al., 2021; Gao et al., 2024).

412

413 4.2 Driving factors of the change in fungal and bacterial necromass contribution to
414 SOC and their ratio

415 Deng and Liang (2022) suggested that the potential contribution of microbial

416 necromass to the SOC pool was governed by the C/N ratio. This finding was
417 confirmed by our results (Figures 4b–d). As elaborated in *Section 4.1*, high N
418 availability (i.e., low soil C/N ratio) promotes the production and accumulation of
419 microbial necromass (Wu et al., 2025). Consequently, the contributions of both FNC
420 and BNC to SOC decreased with increasing soil C/N ratio (Figures S6g, S7g). In
421 agricultural ecosystems, high soil N levels primarily result from fertilization (Chen et
422 al., 2020). In contrast, natural ecosystems experience minimal anthropogenic
423 disturbance, N often acts as the key limiting factor for microbial activity (Elser et al.,
424 2007). Under N-limited conditions, microbes (both fungi and bacteria) allocate more
425 energy and C resources to the synthesis of N-acquiring enzymes (e.g., proteases and
426 chitinases). This shift in metabolic strategy reduces the C allocated to biomass
427 synthesis, thereby diminishing the amount of C ultimately converted into microbial
428 necromass (Mooshammer et al., 2014; Liu et al., 2024). Thus, although microbial
429 community composition differs between natural and agricultural ecosystems, the
430 regulatory role of soil C/N ratio in shaping their structure and function remains
431 consistent (Han et al., 2024). In our study, soil clay content was identified as the
432 predominant factor governing the contribution of FNC to SOC in agricultural
433 ecosystems (Figure 4a), with this contribution increasing concomitantly with clay
434 content (Figure S6d). This suggests that soils with higher clay and silt contents
435 generally accumulate greater amounts of microbial residues, particularly those derived
436 from fungi, which can be attributed to the promotion of stable organo-mineral
437 complex formation by abundant fine soil particles (Six et al., 2006 and Liang et al.,
438 2017). Furthermore, although agricultural management practices often disturb soil
439 structure, they simultaneously enhance clay enrichment and aggregate formation,
440 thereby providing effective physical protection for the long-term stabilization of
441 fungal-derived C (Chen et al., 2020; Mou et al., 2021; Zhou et al., 2023).

442 On the contrary, geographical factor (elevation) was identified as the most
443 influential predictor of the FNC/BNC ratio in both agricultural and natural ecosystems
444 (Figures 4e, f, 5f, 6f), with the ratio increasing significantly with elevation (Figure
445 S8a). Increasing elevation typically leads to decreased temperature, and increased
446 precipitation (Körner, 2007), conditions favoring fungi over bacteria due to higher
447 enzymatic capabilities and resource-use efficiency of fungi under the environments
448 (Chen et al., 2020; Yu et al., 2022; Zhang et al., 2025). High elevation also results in
449 slower soil development, which can reduce the availability of soil nutrients
450 (Guerrero-Ramírez et al., 2020). This in turn increases environmental stress and
451 restricts bacterial activity, thereby favoring the accumulation and conversion of fungal
452 residues into necromass (Li et al., 2024). Our study further demonstrated that although
453 elevation had a direct effect on the FNC/BNC ratio, it also indirectly influenced the
454 ratio by modulating climatic factors, soil physicochemical properties, and biological
455 factors (Figures 5e, 6e). This may explain why elevation is always integrate other
456 environmental factor effects in the studies of MNC (Cui et al., 2023; Zhang et al.,
457 2025).

458
459 4.3 Limitations and uncertainties

460 Although the present study provides important insights on global patterns and drivers
461 of soil microbial necromass in agricultural and natural ecosystems, we must clarify
462 three limitations. First, the limited data available on microbial characteristics, such as
463 microbial community composition, enzymatic activities, and the content of soil
464 aggregates and minerals hinder exploration of the drivers of soil microbial necromass.
465 Second, it is undeniable that our dataset is unevenly distributed, primarily
466 concentrating on the Northern Hemisphere, with sparse or nearly no data from other
467 regions such as Africa, South America, and Australia (Figure 1). Additionally, the
468 natural ecosystems in this study were limited to forests and grasslands, excluding
469 other natural habitats such as wetlands and deserts. The uneven distribution of data
470 may reduce the universality of MNC as a key driver of soil carbon pools in global
471 terrestrial ecosystems. Furthermore, the compiled studies employed varied
472 methodologies regarding sampling time, depth, and laboratory protocols. While such
473 heterogeneity is an inherent challenge in global meta-analyses, it likely introduces
474 additional variability and may constrain the direct comparability of certain data points.
475 Therefore, more standardized data from these important areas and biomes are clearly
476 required, and further investigation is warranted to fill the data gaps regarding the
477 contribution of MNC to SOC in terrestrial ecosystems.

478

479 **5 Data availability**

480 The data and R code for this manuscript are available at
481 <https://doi.org/10.6084/m9.figshare.28827383> (Lu, 2025).

482

483 **6 Conclusions**

484 Our results indicate that, on average, fungal necromass carbon (FNC) contributes
485 approximately twice as much to soil organic carbon (SOC) as bacterial necromass
486 carbon (BNC) in both agricultural and natural ecosystems. The relative contributions
487 of FNC and BNC to SOC were found to be higher in agricultural ecosystems—an
488 effect that is mediated by differences in soil physicochemical factors. The FNC/BNC
489 ratio was significantly higher in natural ecosystems than in agricultural ecosystems,
490 albeit with a modest effect size, and was primarily driven by geographical
491 factors—particularly elevation. Our findings demonstrate that, despite considerable
492 variability among individual sampling sites, statistically significant differences exist
493 between agricultural and natural ecosystems in the contributions of fungal and
494 bacterial necromass carbon (FNC and BNC) to soil organic carbon (SOC), as well as
495 in the FNC/BNC ratio, at a global scale. These results underscore a potential
496 fundamental divergence in the pathways and mechanisms of carbon turnover and
497 stabilization between these two broad ecosystem types. These insights provide novel
498 evidence that ecosystem management type (agricultural versus natural) is a key
499 determinant of the pathways through which microbial necromass contributes to the
500 global soil organic carbon (SOC) pool. Future studies that integrate microbial
501 community composition with necromass dynamics across a broader range of biomes
502 will be essential to predict ecosystem-specific responses of this critical carbon pool to
503 global change.

504

505 **Author contributions**

506 JL performed the data analysis and prepared the original draft. TC and MDB
507 contributed to manuscript review and editing. WL and HS contributed to data
508 collection. YJ contributed to data analysis. ZW supervised the project and contributed
509 to the original draft.

510

511 **Competing interests**

512 The contact author has declared that none of the authors has any competing interests.

513

514 **Disclaimer**

515 Publisher's note: Copernicus Publications remains neutral with regard to jurisdictional
516 claims in published figures and institutional affiliations.

517

518 **Acknowledgements**

519 We are grateful for the data contributors and the scientific community which made the
520 data accessible and useful for our study.

521

522 **Financial support**

523 This work was supported financially by the National Natural Science Foundation of
524 China (No. 32160291), the National Key Research and Development Program of
525 China (No. 2021YFD2200403-04), the Natural Science Foundation of Hainan
526 province (No. 423QN212), the Hainan University Research start-up Fund (No.
527 KYQD(ZR)22187), and the Southwest Minzu University National Huang
528 Danian-style Teacher Team Funding Project (2025).

529

530 **References**

531 Anderson, T. H., and Domsch, K. H.: Ratios of microbial biomass carbon to total
532 organic carbon in arable soils, *Soil Biol. Biochem.*, 21, 471–479,
533 [https://doi.org/10.1016/0038-0717\(89\)90117-X](https://doi.org/10.1016/0038-0717(89)90117-X), 1989.

534 Angst, G., Mueller, K. E., Nierop, K. G., and Simpson, M. J.: Plant-or
535 microbial-derived? A review on the molecular composition of stabilized soil
536 organic matter, *Soil Biol. Biochem.*, 156, 108189,
537 <https://doi.org/10.1016/j.soilbio.2021.108189>, 2021.

538 Bellamy, P. H., Loveland, P. J., Bradley, R. I., Lark, R. M., and Kirk, G. J.: Carbon
539 losses from all soils across England and Wales 1978–2003, *Nature*, 437, 245–248,
540 <https://doi.org/10.1038/nature04038>, 2005.

541 Bohan, D. A., Raybould, A., Mulder, C., Woodward, G., Tamaddoni-Nezhad, A.,
542 Bluthgen, N., Pocock, M. J. O., Muggleton, S., Evans, D. M., Astegiano, J.,
543 Massol, F., Loeuille, N., Petit, S., and Macfadyen, S.: Networking agroecology:
544 integrating the diversity of agroecosystem interactions, *Adv. Ecol. Res.*, 49, 1–67,
545 <https://doi.org/10.1016/B978-0-12-420002-9.00001-9>, 2013.

546 Campitelli, E.: *ggnewscale*: Multiple Fill and Colour Scales in 'ggplot2', R package
547 version 0.4.8., <https://CRAN.R-project.org/package=ggnewscale>, 2022.

548 Cao, Y., Ding, J., Li, J., Xin, Z., Ren, S., and Wang, T.: Necromass-derived soil
549 organic carbon and its drivers at the global scale, *Soil Biol. Biochem.*, 181,
550 109025, <https://doi.org/10.1016/j.soilbio.2023.109025>, 2023.

551 Castellano, M. J., Mueller, K. E., Olk, D. C., Sawyer, J. E., and Six, J.: Integrating
552 plant litter quality, soil organic matter stabilization, and the carbon saturation
553 concept, *Global Change Biol.*, 21, 3200–3209, <https://doi.org/10.1111/gcb.12982>,
554 2015.

555 Chen, G., Ma, S., Tian, D., Xiao, W., Jiang, L., Xing, A., Zou, A., Zhou, L., Shen, H.,
556 Zheng, C., Ji, C., He, H., Zhu, B., Liu, L., and Fang, J.: Patterns and
557 determinants of soil microbial residues from tropical to boreal forests, *Soil Biol.*
558 *Biochem.*, 151, 108059, <https://doi.org/10.1016/j.soilbio.2020.108059>, 2020.

559 Chen, X., Hu, Y., Xia, Y., Zheng, S., Ma, C., Rui, Y., He, H., Huang, D., Zhang, Z., Ge,
560 T., Wu, J., Guggenberger, G., Kuzyakov, Y., and Su, Y.: Contrasting pathways of
561 carbon sequestration in paddy and upland soils, *Global Change Biol.*, 27, 2478–
562 2490, <https://doi.org/10.1111/gcb.15595>, 2021.

563 Choi, J., Bach, E., Lee, J., Flater, J., Dooley, S., Howe, A., and Hofmockel, K. S.:
564 Spatial structuring of cellulase gene abundance and activity in soil, *Front.*
565 *Environ. Sci.*, 6, 107, <https://doi.org/10.3389/fenvs.2018.00107>, 2018.

566 Clocchiatti, A., Hannula, S. E., Hundscheid, M. P., Klein Gunnewiek, P. J., and de
567 Boer, W.: Stimulated saprotrophic fungi in arable soil extend their activity to the
568 rhizosphere and root microbiomes of crop seedlings, *Environ. Microbiol.*, 23,
569 6056–6073, <https://doi.org/10.1111/1462-2920.15563>, 2021.

570 Cotrufo, M. F., Wallenstein, M. D., Boot, C. M., Deneff, K., and Paul, E.: The
571 Microbial Efficiency-Matrix Stabilization (MEMS) framework integrates plant
572 litter decomposition with soil organic matter stabilization: do labile plant inputs
573 form stable soil organic matter?, *Global Change Biol.*, 19, 988–995,
574 <https://doi.org/10.1111/gcb.12113>, 2013.

575 Crowther, T. W., Sokol, N. W., Oldfield, E. E., Maynard, D. S., Thomas, S. M., and
576 Bradford, M. A.: Environmental stress response limits microbial necromass
577 contributions to soil organic carbon, *Soil Biol. Biochem.*, 85, 153–161,
578 <https://doi.org/10.1016/j.soilbio.2015.03.002>, 2015.

579 Cui, W., Li, R., Fan, Z., Wu, L., Zhao, X., Wei, G., and Shu, D.: Weak environmental
580 adaptation of rare phylotypes sustaining soil multi-element cycles in response to
581 decades-long fertilization, *STOTEN.*, 871, 162063,
582 <https://doi.org/10.1016/j.scitotenv.2023.162063>, 2023.

583 de Boer, W. D., Folman, L. B., Summerbell, R. C., and Boddy, L.: Living in a fungal
584 world: impact of fungi on soil bacterial niche development, *FEMS Microbiol.*
585 *Rev.*, 29, 795–811, <https://doi.org/10.1016/j.femsre.2004.11.005>, 2005.

586 Deng, F., and Liang, C.: Revisiting the quantitative contribution of microbial
587 necromass to soil carbon pool: stoichiometric control by microbes and soil, *Soil*
588 *Biol. Biochem.*, 165, 108486, <https://doi.org/10.1016/j.soilbio.2021.108486>,
589 2022.

590 Ding, Z., Mou, Z., Li, Y., Liang, C., Xie, Z., Wang, J., Hui, D., Lambers, H., Sardans,
591 J., Peñuelas, J., Xu, H., and Liu, Z.: Spatial variation and controls of soil

592 microbial necromass carbon in a tropical montane rainforest, *STOTEN.*, 921,
593 170986, <https://doi.org/10.1016/j.scitotenv.2024.170986>, 2024.

594 Elser, J. J., Bracken, M. E., Cleland, E. E., Gruner, D. S., Harpole, W. S., Hillebrand,
595 H., Ngai, J. T., Seabloom, E. W., Shurin, J. B., and Smith, J. E.: Global analysis
596 of nitrogen and phosphorus limitation of primary producers in freshwater, marine
597 and terrestrial ecosystems, *Ecol. Lett.*, 10, 1135–1142,
598 <https://doi.org/10.1111/j.1461-0248.2007.01113.x>, 2007.

599 Fanin, N., Bezaud, S., Sarneel, J. M., Cecchini, S., Nicolas, M., and Augusto, L.:
600 Relative importance of climate, soil and plant functional traits during the early
601 decomposition stage of standardized litter, *Ecosystems*, 23, 1004–1018,
602 <https://doi.org/10.1007/s10021-019-00452-z>, 2020.

603 Gao, W., Duan, X., Chen, X., Wei, L., Wang, S., Wu, J., and Zhu, Z.: Iron-carbon
604 complex types and bonding forms jointly control organic carbon mineralization
605 in paddy soils, *STOTEN.*, 953, 176117,
606 <https://doi.org/10.1016/j.scitotenv.2024.176117>, 2024.

607 Ghezzehei, T. A., Sulman, B., Arnold, C. L., Bogie, N. A., and Berhe, A. A.: On the
608 role of soil water retention characteristic on aerobic microbial respiration,
609 *BIOGEOSCIENCES.*, 16, 1187–1209, <https://doi.org/10.5194/bg-16-1187-2019>,
610 2019.

611 Greenwell, B., Boehmke, B., Cunningham, J., and Developers, G. B. M.: *gbm*:
612 Generalized Boosted Regression Models, R package version 2.1.8.1.,
613 <https://CRAN.R-project.org/package=gbm>, 2022.

614 Han, B., Yao, Y., Wang, Y., Su, X., Ma, L., Chen, X., and Li, Z.: Microbial traits
615 dictate soil necromass accumulation coefficient: A global synthesis, *Global Ecol.*
616 *Biogeogr.*, 33, 151–161, <https://doi.org/10.1111/geb.13776>, 2024.

617 Hao, Z., Zhao, Y., Wang, X., Wu, J., Jiang, S., Xiao, J., Wang, K., Zhou, X., Liu, H., Li,
618 J., and Sun, Y.: Thresholds in aridity and soil carbon-to-nitrogen ratio govern the
619 accumulation of soil microbial residues, *Commun. Earth Environ.*, 2, 236,
620 <https://doi.org/10.1038/s43247-021-00306-4>, 2021.

621 Hättenschwiler, S., Tiunov, A. V., and Scheu, S.: Biodiversity and litter decomposition
622 in terrestrial ecosystems, *Annu. Rev. Ecol. Evol. Syst.*, 36, 191–218,
623 <https://doi.org/10.1146/annurev.ecolsys.36.112904.151932>, 2005.

624 Hobbs, R. J., Hallett, L. M., Ehrlich, P. R., and Mooney, H. A.: Intervention ecology:
625 applying ecological science in the twenty-first century, *BioScience*, 61, 442–450,
626 <https://doi.org/10.1525/bio.2011.61.6.6>, 2011.

627 Hollister, J. W.: *elevatr*: Access Elevation Data from Various APIs, R package version
628 0.4.2., <https://CRAN.R-project.org/package=elevatr/>, 2021.

629 Kallenbach, C. M., Frey, S. D., and Grandy, A. S.: Direct evidence for
630 microbial-derived soil organic matter formation and its ecophysiological controls,
631 *Nat. Commun.*, 7, 13630, <https://doi.org/10.1038/ncomms13630>, 2016.

632 Kassambara, A.: *ggpubr*: 'ggplot2' Based Publication Ready Plots, R package version
633 0.5.0., <https://CRAN.R-project.org/package=ggpubr>, 2022.

634 Keith, D. A., Ferrer-Paris, J. R., Nicholson, E., Bishop, M. J., Polidoro, B. A.,
635 Ramirez-Llodra, E., Tozer, M. G., Nel, J. L., Nally, R. M., Gregr, E. J.,

636 Watermeyer, K. E., Essl, F., Faber-Langendoen, D., Franklin, J., Lehmann, C. E.
637 R., Etter, A., Roux, D. J., Stark, J. S., Rowland, J. A., Brummitt, N. A.,
638 Fernandez-Arcaya, U. C., Suthers, I. M., Wisser, S. K., Donohue, I., Jackson, L. J.,
639 Pennington, R. T., Iliffe, T. M., Gerovasileiou, V., Giller, P., Robson, B. J.,
640 Pettorelli, N., Andrade, A., Lindgaard, A., Tahvanainen, T., Terauds, A.,
641 Chadwick, M. A., Murray, N. J., Moat, J., Pliscoff, P., Zager, I., and Kingsford, R.
642 T.: A function-based typology for Earth's ecosystems, *Nature*, 610, 513–518,
643 <https://doi.org/10.1038/s41586-022-05318-4>, 2022.

644 Kleber, M., Bourg, I. C., Coward, E. K., Hansel, C. M., Myneni, S. C., and Nunan, N.:
645 Dynamic interactions at the mineral–organic matter interface, *NAT REV EARTH*
646 *ENV.*, 2, 402–421, <https://doi.org/10.1038/s43017-021-00162-y>, 2021.

647 Klink, S., Keller, A. B., Wild, A. J., Baumert, V. L., Gube, M., Lehndorff, E., Meyer,
648 N., Mueller, C. W., Phillips, R. P., and Pausch, J.: Stable isotopes reveal that
649 fungal residues contribute more to mineral-associated organic matter pools than
650 plant residues, *Soil Biol. Biochem.*, 168, 108634,
651 <https://doi.org/10.1016/j.soilbio.2022.108634>, 2022.

652 Kock, N.: Common method bias in PLS-SEM: A full collinearity assessment approach,
653 *International Journal of e-Collaboration (IJeC)*, 11, 1–10,
654 <https://doi.org/10.4018/ijec.2015100101>, 2015.

655 Körner, C.: The use of ‘altitude’ in ecological research, *Trends Ecol. Evol.*, 22, 569–
656 574, <https://doi.org/10.1016/j.tree.2007.09.006>, 2007.

657 Lembrechts, J. J., van den Hoogen, J., Aalto, J., Ashcroft, M. B., De Frenne, P.,
658 Kemppinen, J., Kopecký, M., Luoto, Maclean, M. I. M. D., Crowther, T. W.,
659 Bailey, J. J., Haesen, S., Klinges, D. H., Niittynen, P., Scheffers, B. R., Van
660 Meerbeek, K., Aartsma, P., Abdalaze, O., Abedi, M., Aerts, R., Ahmadian, N.,
661 Ahrends, A., Alatalo, J. M., Alexander, J. M., Allonsius, C. N., Altman, J.,
662 Ammann, C., Andres, C., Andrews, C., Ardö, J., Arriga, N., Arzac, A., Aschero,
663 V., Assis, R. L., Assmann, J. J., Bader, M. Y., Bahalkeh, K., Barančok, P., Barrio,
664 I. C., Barros, A., Barthe, M., Basham, E. W., Bauters, M., Bazzichetto, M.,
665 Marchesini, L. B., Bell, M. C., Benavides, J. C., Alonso, J. L. B., Berauer, B. J.,
666 Bjerke, J. W., Björk, R. G., Björkman, M. P., Björnsdóttir, K., Blonder, B.,
667 Boeckx, P., Boike, J., Bokhorst, S., Brum, B. N. S., Bruna, J., Buchmann, N.,
668 Buysse, P., Camargo, J. L., Campoe, O. C., Candan, O., Canessa, R., Cannone,
669 N., and Hik, D. S.: Global maps of soil temperature, *Global Change Biol.*, 28,
670 3110–3144, <https://doi.org/10.1111/gcb.16060>, 2022.

671 Lehmann, J., Hansel, C. M., Kaiser, C., Kleber, M., Maher, K., Manzoni, S., Nunan,
672 N., Reichstein, M., Schimel, J. P., Torn, M. S., Wieder, W. R., and
673 Kögel-Knabner, I.: Persistence of soil organic carbon caused by functional
674 complexity, *Nat. Geosci.*, 13, 529–534,
675 <https://doi.org/10.1038/s41561-020-0612-3>, 2020.

676 Lenardon, M. D., Whitton, R. K., Munro, C. A., Marshall, D., and Gow, N. A. R.:
677 Individual chitin synthase enzymes synthesize microfibrils of differing structure
678 at specific locations in the *Candida albicans* cell wall, *Mol. Microbiol.*, 66,
679 1164–1173, <https://doi.org/10.1111/j.1365-2958.2007.05990.x>, 2007.

680 Liang, C., Amelung, W., Lehmann, J., and Kästner, M.: Quantitative assessment of
681 microbial necromass contribution to soil organic matter, *Global Change Biol.*, 25,
682 3578–3590, <https://doi.org/10.1111/gcb.14781>, 2019.

683 Liang, C., and Balser, T. C.: Microbial production of recalcitrant organic matter in
684 global soils: implications for productivity and climate policy, *Nat. Rev.*
685 *Microbiol.*, 9, 75–75, <https://doi.org/10.1038/nrmicro2386-c1>, 2011.

686 Liang, C., Schimel, J. P., and Jastrow, J. D.: The importance of anabolism in microbial
687 control over soil carbon storage, *Nat. Microbiol.*, 2, 17105,
688 <https://doi.org/10.1038/nmicrobiol.2017.105>, 2017.

689 Liu, C., Tian, J., Cheng, K., Xu, X., Wang, Y., Liu, X., Liu, Z., Bian, R., Zhang, X.,
690 Xia, S., Zheng, J., Li, L., and Pan, G.: Topsoil microbial biomass carbon pool
691 and the microbial quotient under distinct land-use types across China: A data
692 synthesis, *SSE.*, 2, 5, <https://doi.org/10.48130/SSE-2023-0005>, 2023.

693 Liu, X., Tian, Y., Heinzle, J., Salas, E., Kwatcho-Kengdo, S., Borken, W.,
694 Schindlbacher, A., and Wanek, W.: Long-term soil warming decreases soil
695 microbial necromass carbon by adversely affecting its production and
696 decomposition, *Global Change Biol.*, 30, e17379,
697 <https://doi.org/10.1111/gcb.17379>, 2024.

698 Li, Y., Wang, S., Yang, Y., Ren, L., Wang, Z., Liao, Y., and Yong, T.: Global synthesis
699 on the response of soil microbial necromass carbon to climate-smart agriculture,
700 *Global Change Biol.*, 30(5), e17302, <https://doi.org/10.1111/gcb.17302>, 2024.

701 Lu, J.: Microbial necromass contribution to topsoil organic carbon storage of natural
702 and agricultural ecosystems, *figshare* [data set],
703 <https://doi.org/10.6084/m9.figshare.28827383>, 2025.

704 Luo, R., Kuzyakov, Y., Zhu, B., Qiang, W., Zhang, Y., and Pang, X.: Phosphorus
705 addition decreases plant lignin but increases microbial necromass contribution to
706 soil organic carbon in a subalpine forest, *Global Change Biol.*, 28, 4194–4210,
707 <https://doi.org/10.1111/gcb.16205>, 2022.

708 Malik, A. A., Chowdhury, S., Schlager, V., Oliver, A., Puissant, J., Vazquez, P. G.,
709 Jehmlich, N., von Bergen, M., Griffiths, R., and Gleixner, G.: Soil fungal:
710 bacterial ratios are linked to altered carbon cycling, *Front. Microbiol.*, 7, 1247,
711 <https://doi.org/10.3389/fmicb.2016.01247>, 2016.

712 Ma, T., Zhu, S., Wang, Z., Chen, D., Dai, G., Feng, B., Su, X., Hu, H., Li, K., Han, W.,
713 Liang, C., Bai, Y., and Feng, X.: Divergent accumulation of microbial necromass
714 and plant lignin components in grassland soils, *Nat. Commun.*, 9, 3480,
715 <https://doi.org/10.1038/s41467-018-05891-1>, 2018.

716 Mooshammer, M., Wanek, W., Zechmeister-Boltenstern, S., and Richter, A.:
717 Stoichiometric imbalances between terrestrial decomposer communities and their
718 resources: mechanisms and implications of microbial adaptations to their
719 resources, *Front. Microbiol.*, 5, 22, <https://doi.org/10.3389/fmicb.2014.00022>,
720 2014.

721 Mou, Z., Kuang, L., He, L., Zhang, J., Zhang, X., Hui, D., Li, Y., Wu, W., Mei, Q., He,
722 X., Kuang, Y., Wang, J., Wang, Y., Lambers, H., Sardans, J., Peñuelas, J., and Liu,
723 Z.: Climatic and edaphic controls over the elevational pattern of microbial

724 necromass in subtropical forests, *Catena*, 207, 105707,
725 <https://doi.org/10.1016/j.catena.2021.105707>, 2021.

726 Ni, X., Liao, S., Tan, S., Peng, Y., Wang, D., Yue, K., Wu, F., and Yang, Y.: The
727 vertical distribution and control of microbial necromass carbon in forest soils,
728 *Global Ecol. Biogeogr.*, 29, 1829–1839, <https://doi.org/10.1111/geb.13159>, 2020.

729 Oksanen, J., Blanchet, F. G., Friendly, M., Kindt, R., Legendre, P., McGlinn, D., and
730 Wagner, H.: *vegan*: Community Ecology Package, R package version 2.5.7.,
731 <https://CRAN.R-project.org/package=vegan>, 2020.

732 Poggio, L., De Sousa, L. M., Batjes, N. H., Heuvelink, G., Kempen, B., Ribeiro, E.,
733 and Rossiter, D.: SoilGrids 2.0: producing soil information for the globe with
734 quantified spatial uncertainty, *Soil*, 7, 217–240,
735 <https://doi.org/10.5194/soil-7-217-2021>, 2021.

736 Qiu, H., Zheng, X., Ge, T., Dorodnikov, M., Chen, X., Hu, Y., Kuzyakov, Y., Wu, J.,
737 Su, Y., and Zhang, Z.: Weaker priming and mineralisation of low molecular
738 weight organic substances in paddy than in upland soil, *Eur. J. Soil Biol.*, 83, 9–
739 17, <https://doi.org/10.1016/j.ejsobi.2017.09.008>, 2017.

740 R Core Team: R: A language and environment for statistical computing, R Foundation
741 for Statistical Computing, Vienna, Austria, <https://www.R-project.org>, 2021.

742 Rosseel, Y.: *lavaan*: An R package for structural equation modeling, *J. Stat. Softw.*, 48,
743 1–36, <https://doi.org/10.18637/jss.v048.i02>, 2012.

744 Sae-Tun, O., Bodner, G., Rosinger, C., Zechmeister-Boltenstern, S., Mentler, A., and
745 Keiblinger, K.: Fungal biomass and microbial necromass facilitate soil carbon
746 sequestration and aggregate stability under different soil tillage intensities, *Appl.*
747 *Soil Ecol.*, 179, 104599, <https://doi.org/10.1016/j.apsoil.2022.104599>, 2022.

748 Sanaullah, M., Usman, M., Wakeel, A., Cheema, S. A., Ashraf, I., and Farooq, M.:
749 Terrestrial ecosystem functioning affected by agricultural management systems:
750 A review, *Soil Tillage Res.*, 196, 104464,
751 <https://doi.org/10.1016/j.still.2019.104464>, 2020.

752 Six, J., Frey, S. D., Thiet, R. K., and Batten, K. M.: Bacterial and fungal contributions
753 to carbon sequestration in agroecosystems, *Soil Sci. Soc. Am. J.*, 70, 555–569,
754 <https://doi.org/10.2136/sssaj2004.0347>, 2006.

755 Spawn, S. A., Sullivan, C. C., Lark, T. J., and Gibbs, H. K.: Harmonized global maps
756 of above and belowground biomass carbon density in the year 2010, *Sci. Data*, 7,
757 112, <https://doi.org/10.1038/s41597-020-0444-4>, 2020.

758 Strickland, M. S., and Rousk, J.: Considering fungal: bacterial dominance in soils–
759 methods, controls, and ecosystem implications, *Soil Biol. Biochem.*, 42, 1385–
760 1395, <https://doi.org/10.1016/j.soilbio.2010.05.007>, 2010.

761 Štursová, M., Žifčáková, L., Leigh, M. B., Burgess, R., and Baldrian, P.: Cellulose
762 utilization in forest litter and soil: identification of bacterial and fungal
763 decomposers, *FEMS Microbiol. Ecol.*, 80, 735–746.
764 <https://doi.org/10.1111/j.1574-6941.2012.01343.x>, 2012.

765 van Der Heijden, M. G., Bardgett, R. D., and van Straalen, N. M.: The unseen
766 majority: soil microbes as drivers of plant diversity and productivity in terrestrial

767 ecosystems, Ecol. Lett., 11, 296–310,
768 <https://doi.org/10.1111/j.1461-0248.2007.01139.x>, 2008.

769 Wang, B., An, S., Liang, C., Liu, Y., and Kuzyakov, Y.: Microbial necromass as the
770 source of soil organic carbon in global ecosystems, *Soil Biol. Biochem.*, 162,
771 108422, <https://doi.org/10.1016/j.soilbio.2021.108422>, 2021a.

772 Wang, B., Liang, C., Yao, H., Yang, E., and An, S.: The accumulation of microbial
773 necromass carbon from litter to mineral soil and its contribution to soil organic
774 carbon sequestration, *Catena*, 207, 105622,
775 <https://doi.org/10.1016/j.catena.2021.105622>, 2021b.

776 Wang, C., and Kuzyakov, Y.: Mechanisms and implications of bacterial–fungal
777 competition for soil resources, *ISME J.*, 18, wrac073,
778 <https://doi.org/10.1093/ismejo/wrac073>, 2024.

779 Wang, Z., Zhao, M., Yan, Z., Yang, Y., Niklas, K. J., Huang, H., Mipam, T. D., He, X.,
780 Hu, H., and Wright, S. J.: Global patterns and predictors of soil microbial
781 biomass carbon, nitrogen, and phosphorus in terrestrial ecosystems, *Catena*, 211,
782 106037, <https://doi.org/10.1016/j.catena.2022.106037>, 2022.

783 Wickham, H.: *ggplot2: elegant graphics for data analysis*. Springer-Verlag New York,
784 <https://ggplot2.tidyverse.org>, 2016.

785 Wu, H., Xiang, W., Ouyang, S., Forrester, D. I., Zhou, B., Chen, L., Ge, T., Lei, P.,
786 Chen, L., Zeng, Y., Song, X., Peñuelas, J., and Peng, C.: Linkage between tree
787 species richness and soil microbial diversity improves phosphorus bioavailability,
788 *Funct. Ecol.*, 33, 1549–1560, <https://doi.org/10.1111/1365-2435.13355>, 2019.

789 Wu, W., Feng, J., Wang, X., Xiao, J., Qin, W., and Zhu, B.: The response of soil
790 microbial necromass carbon to global change: A global meta-analysis, *Catena*,
791 249, 108693, <https://doi.org/10.1016/j.catena.2024.108693>, 2025.

792 Xu, S., Song, X., Zeng, H., and Wang, J.: Soil microbial necromass carbon in forests:
793 A global synthesis of patterns and controlling factors, *Soil Ecol. Lett.*, 6(4),
794 240237, <https://doi.org/10.1007/s42832-024-0237-3>, 2024.

795 Xu, Y., Sun, L., Gao, X., and Wang, J.: Contrasting response of fungal versus bacterial
796 residue accumulation within soil aggregates to long-term fertilization, *Sci. Rep.*,
797 12, 17834, <https://doi.org/10.1038/s41598-022-22064-9>, 2022.

798 Yu, K., van den Hoogen, J., Wang, Z., Averill, C., Routh, D., Smith, G. R., Drenovsky,
799 R. E., Scow, K. M., Mo, F., Waldrop, M. P., Yang, Y., Tang, W., Vries, F. T. D.,
800 Bardgett, R. D., Manning, P., Bastida, F., Baer, S. G., Bach, E. M., García, C.,
801 Wang, Q., Ma, L., Chen, B., He, X., Teurlincx, S., Heijboer, A., Bradley, J. A.,
802 and Crowther, T. W.: The biogeography of relative abundance of soil fungi
803 versus bacteria in surface topsoil, *Earth Syst. Sci. Data*, 14, 4339–4350,
804 <https://doi.org/10.5194/essd-14-4339-2022>, 2022.

805 Zhang, B., Zhu, S., Guo, L., Chen, G., Zhang, G., and Li, J.: Elevation-dependent
806 distribution of soil microbial necromass carbon in *Pinus densata* Mast. Forests,
807 *Appl. Soil Ecol.*, 209, 106049, <https://doi.org/10.1016/j.apsoil.2025.106049>,
808 2025.

809 Zhang, Q., Li, X., Liu, J., Liu, J., Han, L., Wang, X., Liu, H., Xu, M., Yang, G., Ren,
810 C., and Han, X.: The contribution of microbial necromass carbon to soil organic

811 carbon in soil aggregates, *Appl. Soil Ecol.*, 190, 104985,
812 <https://doi.org/10.1016/j.apsoil.2023.104985>, 2023.

813 Zhang, X., Jia, J., Chen, L., Chu, H., He, J. S., Zhang, Y., and Feng, X.: Aridity and
814 NPP constrain contribution of microbial necromass to soil organic carbon in the
815 Qinghai-Tibet alpine grasslands, *Soil Biol. Biochem.*, 156, 108213,
816 <https://doi.org/10.1016/j.soilbio.2021.108213>, 2021.

817 Zhao, M., and Running, S. W.: Drought-induced reduction in global terrestrial net
818 primary production from 2000 through 2009, *Science*, 329, 940–943,
819 <https://doi.org/10.1126/science.1192666>, 2010.

820 Zhao, X., Tian, P., Liu, S., Yin, P., Sun, Z., and Wang, Q.: Mean annual temperature
821 and carbon availability respectively controlled the contributions of bacterial and
822 fungal necromass to organic carbon accumulation in topsoil across China's
823 forests, *Global Ecol. Biogeogr.*, 32, 120–131, <https://doi.org/10.1111/geb.13605>,
824 2023.

825 Zhou, R., Liu, Y., Dungait, J. A., Kumar, A., Wang, J., Tiemann, L. K., Zhang, F.,
826 Kuzyakov, Y., and Tian, J.: Microbial necromass in cropland soils: A global
827 meta-analysis of management effects, *Global Change Biol.*, 29, 1998–2014,
828 <https://doi.org/10.1111/gcb.16613>, 2023.

829 **Table 1. Summary of the contributions of fungal necromass carbon (FNC) and**
830 **bacterial necromass carbon (BNC) to SOC and the FNC/BNC ratio in**
831 **agricultural and natural ecosystems at the global scale investigated in this study.**

Ecosystem	FNC/SOC (%)		BNC/SOC (%)		FNC/BNC	
	Range	Mean± SE	Range	Mean± SE	Range	Mean± SE
Natural ecosystem^{&} (<i>N</i> = 341)	0.92– 96.29	29.24 ± 0.51 b*	0.25– 89.45	14.02 ± 0.36 b	0.12– 44.24	3.22 ± 0.11 a
<i>Forest</i> (<i>N</i> = 195)	0.92– 96.29	29.11 ± 0.63 A [#]	0.94– 96.47	13.48 ± 0.43 A	0.22– 11.56	2.80 ± 0.07 A
<i>Grassland</i> (<i>N</i> = 146)	0.96– 93.89	26.75 ± 0.74 A	0.25– 89.45	14.34 ± 0.60 A	0.05– 44.24	3.58 ± 0.22 A
Agricultural ecosystem[%] (<i>N</i> = 145)	0.09– 97.53	34.39 ± 0.67 a	0.81– 65.00	15.65 ± 0.33 a	0.02– 12.74	2.61 ± 0.06 b
<i>Dry land</i> (<i>N</i> = 32)	3.01– 96.81	37.77 ± 1.15 A [#]	0.81– 65.00	17.34 ± 0.65 A	0.13– 9.12	2.87 ± 0.12 A
<i>Irrigated cropland</i> (<i>N</i> = 72)	0.09– 97.25	35.35 ± 0.73 A	1.18– 62.47	15.95 ± 0.38 A	0.02– 12.74	2.51 ± 0.06 A
<i>Submerged paddy</i> (<i>N</i> = 41)	4.96– 97.53	22.82 ± 1.55 B	1.48– 30.97	10.55 ± 0.66 B	0.31– 10.40	2.62 ± 0.16 A

832 Note: *N* refers to the number of study sites;

833 [&]Natural ecosystem includes forest and grassland;

834 [%]Agricultural ecosystem includes dry land, irrigated cropland, and submerged paddy;

835 ^{*}Within the same column, values with different lowercase letters indicate a significant
836 difference in the same variable between agricultural and natural ecosystems
837 (Wilcoxon rank sum test; *P* < 0.05);

838 [#]Within the same column, values with different capital letters indicate a significant
839 difference in the same variable between forests and grasslands (Wilcoxon rank sum
840 test), as well as between dry land, irrigated cropland, and submerged paddy (Kruskal–
841 Wallis and Dunn’s post hoc tests; *P* < 0.05).

842 **Figure legends**

843 **Figure 1. Global distribution of the sites used in this study.** Ecosystem types are
844 distinguished by distinct shapes and colors, with the numbers in parentheses
845 indicating the number of study sites for each ecosystem type.

846 **Figure 2. Comparison of the contributions of MNC to SOC and their ratio in**
847 **agricultural and natural ecosystems.** Colors indicate different ecosystems types.
848 Significance levels: *** $P < 0.001$ and * $P < 0.05$.

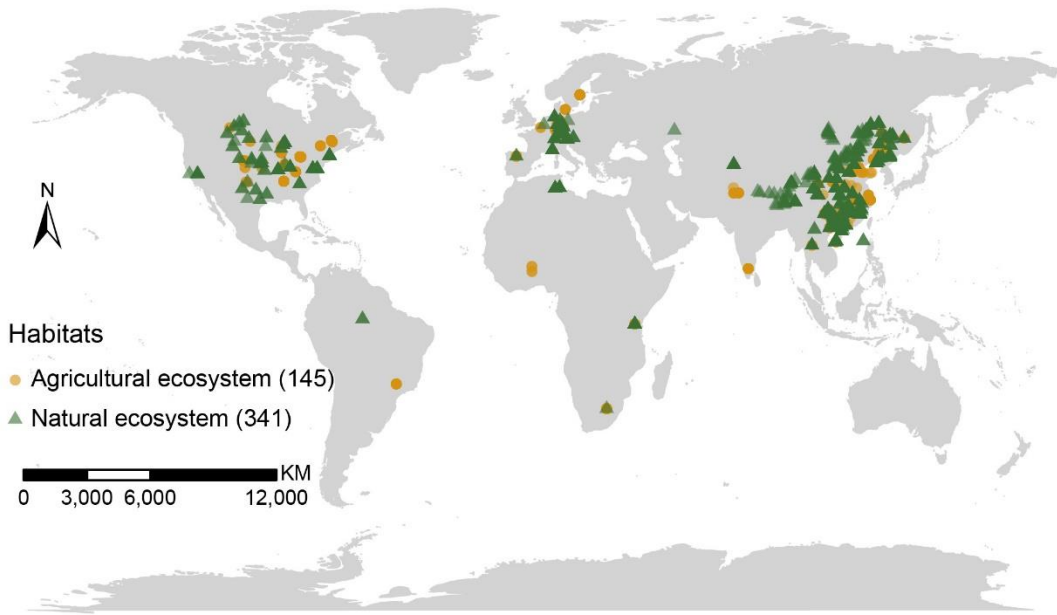
849 **Figure 3. Variations in the contributions of MNC to SOC and their ratio**
850 **explained by four types of factors in agricultural and natural ecosystems.** Colors
851 indicate different types of factors.

852 **Figure 4. Relative influence of different factors on the contributions of MNC to**
853 **SOC and their ratio in agricultural and natural ecosystems.** MAT, mean annual
854 temperature; MAP, mean annual precipitation; MBC, microbial biomass carbon; SOC,
855 soil organic carbon; C/N, the ratio of SOC to total nitrogen (TN); MBC/MBN, the
856 ratio of MBC to microbial biomass nitrogen (MBN); NPP, net primary production;
857 BGBC, belowground biomass carbon density. Colors indicate different types of
858 factors.

859 **Figure 5. The influence pathways of four types of factors on the contributions of**
860 **MNC to SOC and their ratio in agricultural ecosystems.** Direct and indirect effects
861 (a, c, e) and the standardized total effects (b, d, f) of different factors on the
862 contributions of MNC to SOC and their ratio of agricultural ecosystems are shown.
863 Standardized path coefficients representing the effect sizes of potential causal factors
864 are indicated by numbers adjacent to arrows. The width of arrows is proportional to
865 the potential causal effect between variables. The red arrows indicate positive effects,
866 and the blue arrows indicate negative effects. The numbers adjacent to boxes of
867 response variables denote the explained variance (R^2). Right-angled rectangles denote
868 single variables, whereas rounded rectangles represent composite variables. Colors
869 indicate different types of factors. Significance levels: *** $P < 0.001$, ** $P < 0.01$ and
870 * $P < 0.05$. The *priori* models are shown in Figure S3.

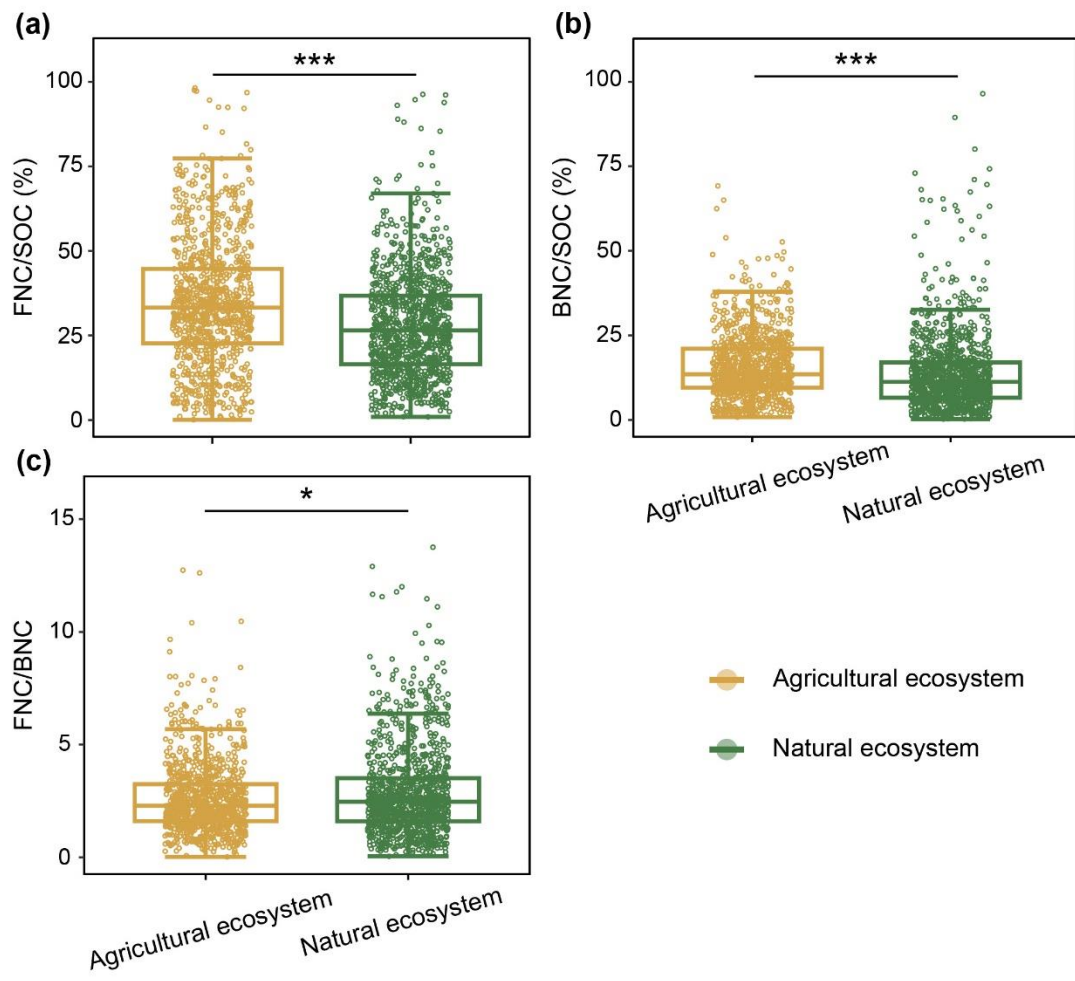
871 **Figure 6. The influence pathways of four types of factors on the contributions of**
872 **MNC to SOC and their ratio in natural ecosystems.** Direct and indirect effects (a, c,
873 e) and the standardized total effects (b, d, f) of different factors on the contributions of
874 MNC to SOC and their ratio of natural ecosystems are shown. Standardized path
875 coefficients representing the effect sizes of potential causal factors are indicated by
876 numbers adjacent to arrows. The width of arrows is proportional to the potential
877 causal effect between variables. The red arrows indicate positive effects, and the blue
878 arrows indicate negative effects. The numbers adjacent to boxes of response variables
879 denote the explained variance (R^2). Right-angled rectangles denote single variables,
880 whereas rounded rectangles represent composite variables. Colors indicate different
881 types of factors. Significance levels: *** $P < 0.001$, ** $P < 0.01$ and * $P < 0.05$. The
882 *priori* models are shown in Figure S3.

883 **Figure 1.**

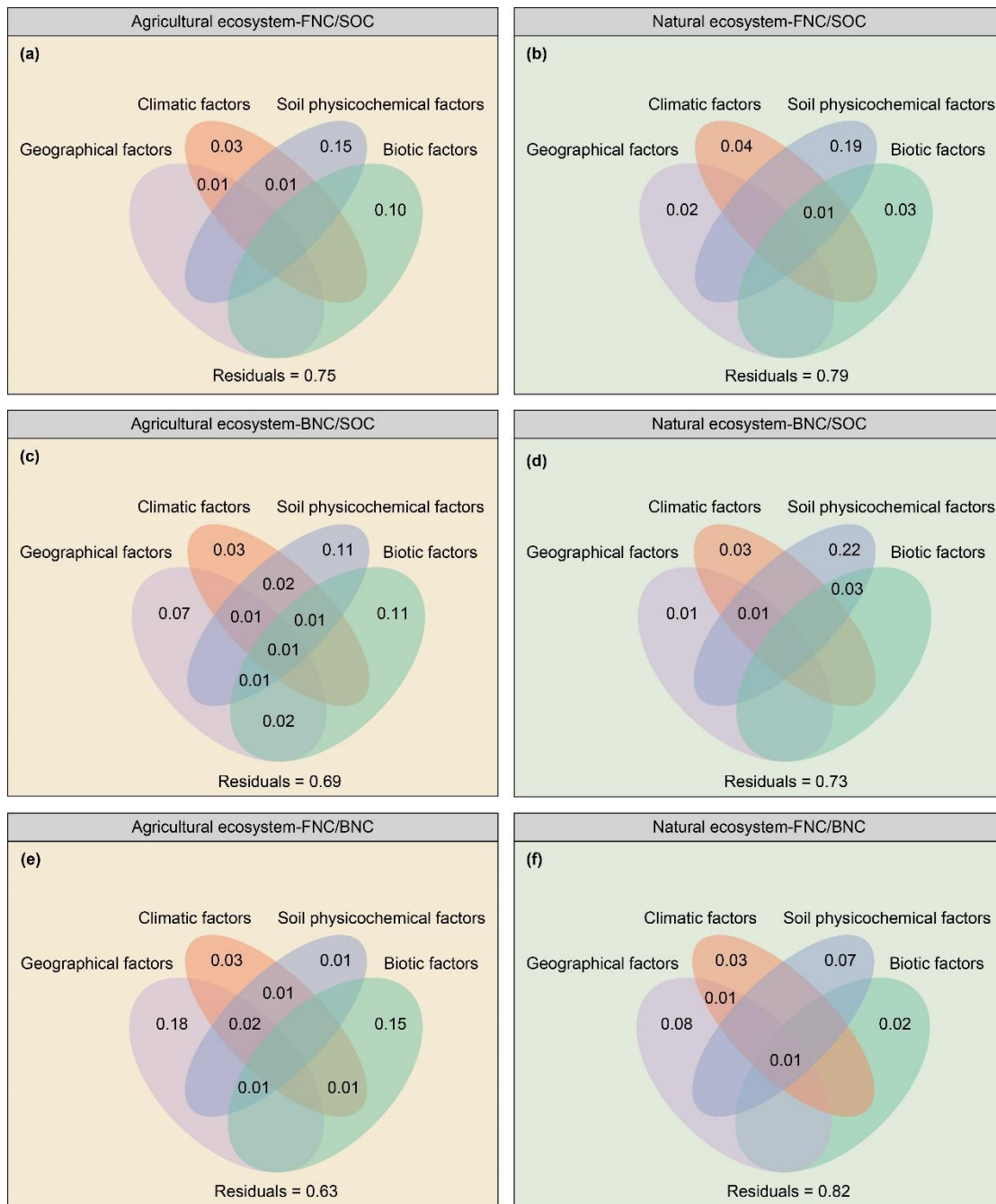


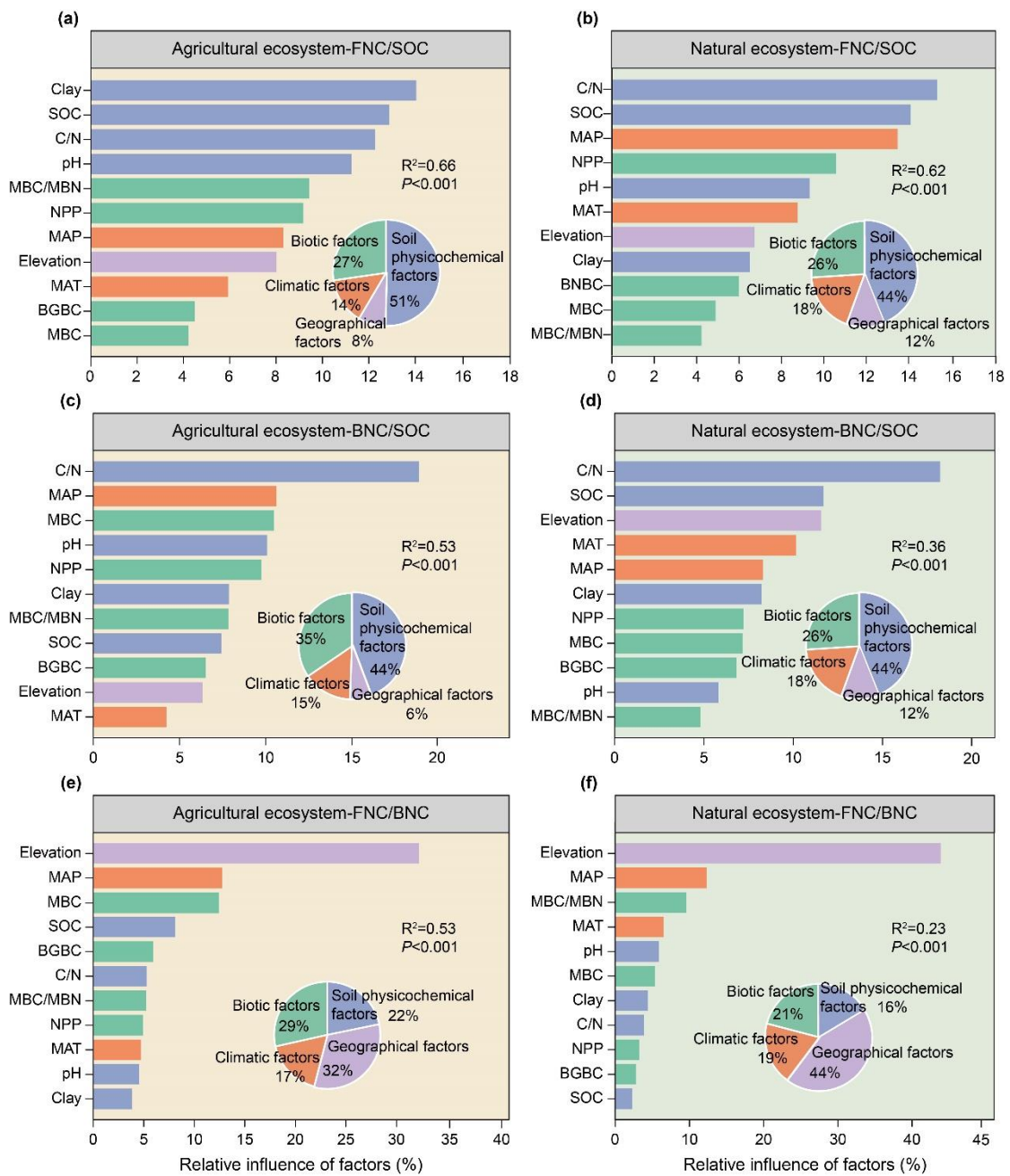
884

885 **Figure 2.**

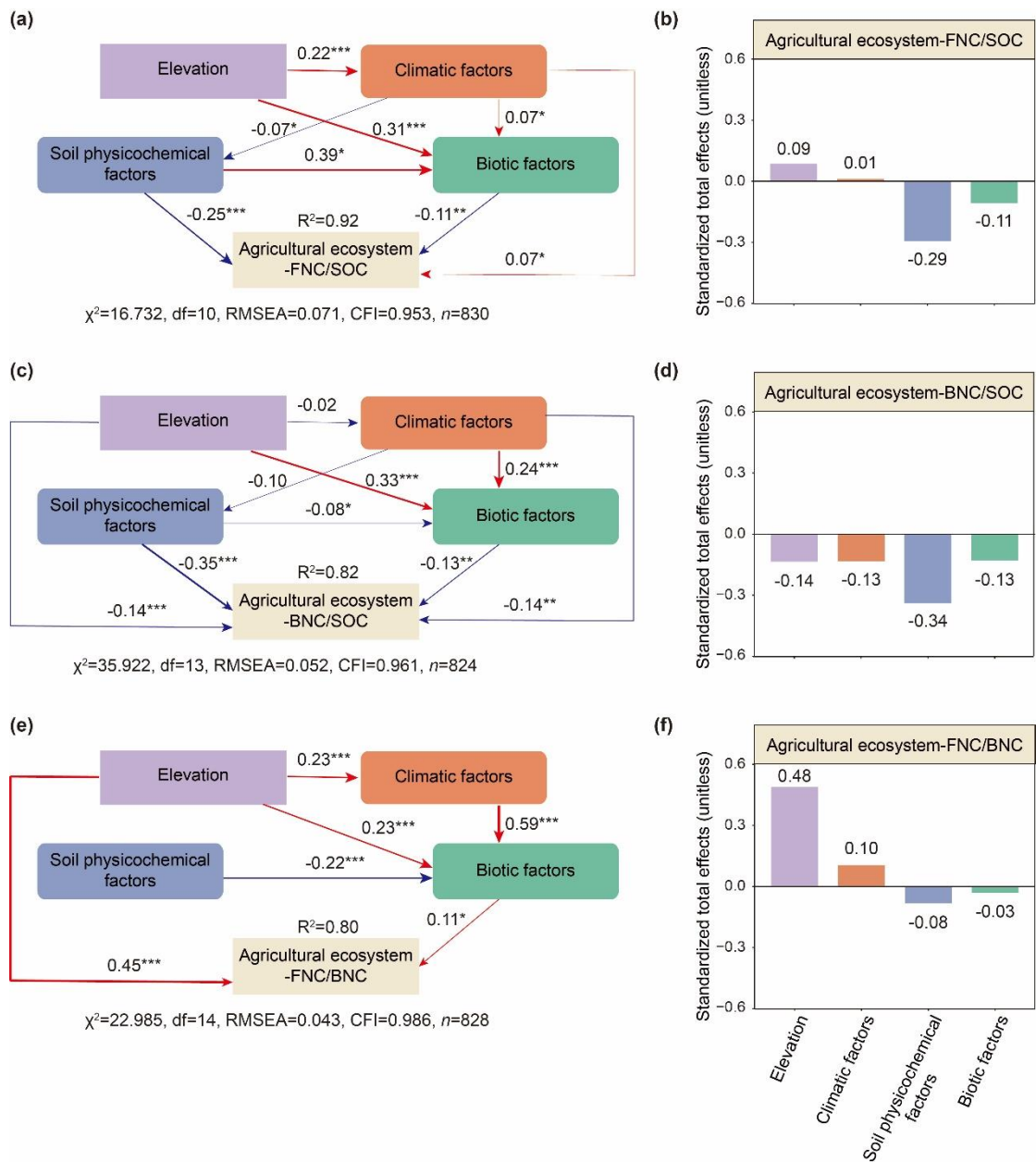


886





891 **Figure 5.**



892

